Engineering Chemistry *Online: 2026-02-18*
ISSN: 2813-6535, Vol. 13, pp 23-38
doi:10.4028/p-9tPQ07

Theoretical and Experimental Study Using Hyperchem-8 and Gaussian Computer Program to Study the Stability, Binding Energies, and Electrical Characteristics of Triazole-Based Metal Complexes in the Gas Phase

Jihan Hameed Abdulameer[1,a], Adnan I. Mohammed[2,b], Mahasin F. Alias[3,c] and Muntahaa Abdullah REISHAAN[4,d]

[1]Department of Chemistry, College of Education for Pure Sciences, University of Kerbala, Iraq.

[2]Department of Chemistry, College of Science, Kerbala University, Karbala, Iraq

[3]Department of Chemistry, College of Science for Women, University of Baghdad, Iraq.

[4]Department of Anesthesia, College Health and Medical Technology, University of Alkafeel Najaf, Iraq

[a]Jihan.hameed@uokerbala.edu.iq, [b]adnan.i@uokerbala.edu.iq, [c]mahasinfa_chem@csw.uobaghdad.edu.iq, [d]muntaha.abd@alkafeel.edu.iq

Keywords: ligand-chelate complexes, Heat of formation, binding energy, and dipole moment, LUMO, HOMO.

Abstract: The study involves treating various metal complexes in "gas phase" with the prepared ligands (2,6-bis(((1-octyl-1H-1,2,3-triazol-4-yl) methoxy) methyl) pyridine (L_1), 2,6-bis(((1-decyl-1H-1,2,3-triazol-4-yl) methoxy) methyl) pyridine (L_2) and 2,6-bis(((1-dodecyl-1H-1,2,3-triazol-4-yl)methoxy) methyl) pyridine (L_3). Two different types of programs, the Hyperchem-8 and Gaussian programs, were used to study the theory. The heat of formation ($\Delta H^o f$), binding energy (ΔEb), and dipole moment (μ) for free ligands and some metal complexes were calculated using semi-experimental and molecular mechanics in the Hyper-8 program using a variety of computational techniques including ZINDO/1, PM3, and AMBER methods at room temperature. The created complexes are discovered to be more stable than the free ligands. For proper location of the molecules, Hyperchem.-8 was used to determine the vibration frequencies for (FT-IR) and electronic transitions, as well as electrostatic potential, HOMO, and LUMO energy. The compatibility of the theoretical and experimental findings was highlighted. In order to calculate the geometry optimization, dipole moment (μ), total energy, electrostatic potential, LUMO, and HOMO, a Gaussian algorithm employing a semi-empirical (PM3) approach was utilized. "Vibration spectra of free ligands are calculated and noted that they agreed well with those values experimentally found" diagnosis with a higher level of capacity to effectively diagnose packages. Using a technique like ZINDO/S, the electronic transitions for the ligand were also computed.

1. Introduction

In the past ten years, quantum computing has been extensively used to address a range of difficult mathematical problems connected to quantum physics, following significant commercial breakthroughs in the field [1]. The computer industry and its software have helped many researchers find atoms and compounds that were challenging or impossible to study. Many research projects employing ever-evolving computer software have been used to discover it [2]. The theoretical study that is the subject of our examination is one of the most significant investigations carried out today because it is totally based on theoretical concerns [3]. Because the investigation was carried out using a computer and an application, it might be regarded as a simulated experiment. This kind of research has demonstrated its value in precisely reproducing material properties, excluding a few mistakes [4,5]. Using two semi-experimental programs, Hyper-Chem and Gaussian computation of the prepared bonds with various metal complexes [6,7,8], our theoretical research will concentrate on investigating these compounds theoretically in the gas phase in order to: - Calculate the heat of

formation (ΔH°f), binding energy (ΔEb), and dipole moment (μ) for each potential geometry and display the best stable conformation. The most active ligands are identified and their HOMO and LUMO positions are displayed using electron potential (Ep) calculations. Set the majority of the diagnostic ranges with certainty by computing the electronic transition and vibration frequencies of the associations and comparing the findings to the experimental transition and vibration frequencies[9,10].

2 Materials and Methods

Theoretical treatment

(2-1) Programs used Hyperchem and Gaussian in theoretical calculation:

(2-1-1) Types of calculation:

In recent years, Hyperchem and Gaussian programs have been used in theoretical programs. These programs stand out for their simplicity and adaptability in use, as well as their use with both organic and inorganic compounds and a wide range of metals[11,12].

In this study, the heat of formation, the dipolar bond energy moment, the IR, UV, HOMO, and LUMO calculations for produced ligands, as well as all complexes prepared using the Hyperchem-8 program, were computed.

(2-2) Computational Methods:

(2-2-1) Semi-Empirical:

The heat of formation, binding energy, and dipole moment of metallic bonds and complexes were calculated using Zerner's INDO method (ZINDO/1), PM3, and (ZINDO/S), which is one of the 12 methods that make up the semi-experimental approach[13,14]. PM3 and (ZINDO/S) were used to determine the ligands' electrical and vibrational spectra.

(2-2-2) Molecular Mechanics:

Many variables, such as the number of atoms, the functional form, and the atomic patterns, affect molecular mechanics. The complexes' formation heat, bond energy, and dipole moment were calculated using the Energy Building and Refinement Model (AMBER).

3 Results and Discussion

Theoretical study:

Using two programs, Hyperchem-8 and Gaussian arithmetic, components of heat (ΔH°f), binding energy (ΔEb), dipole moment (μ), vibrational and electronic transmission frequency spectroscopy, molecular orbital energy, and vacant high and low molecular orbitals were determined(EHOMO-ELUMO) [15].

(3-1) Theoretical energies and the dipole moment:

The molecular dipole moment is the only empirical measure of the price density of the molecule. Using the PM3, ZINDO/1, and AMBER methodologies, the heat composition (ΔH°f), binding energy (ΔEb), and dipole moment (μ) of free bonds and their metal complexes were calculated [16,17]. As shown in Table 1, complexes are more stable than free bonds based on the results of using Hyperchem-8.

Table 1. Heat of formation, binding energy (Kcal.mol^{-1}) and dipole moment (in Debye) for all ligands and their metal complexes calculated with Hyperchem-8.

	PM3			ZINDO/1			AMBER
Comp.	**ΔH°f**	**ΔEb**	**μ**	**ΔH°f**	**ΔEb**	**μ**	**ΔH°f =ΔEb**
L_1	-11.8206	-2302.901	8.201	-10322.221	-14636.943	5.23	42.8725
Mn-L_1	-84.272	-8704.092	13.78	-16704.499	-25324.319	5.938	156.312
Ni-L_1	-169.638	-8668.252	7.083	-16866.126	-25364.740	6.593	134.348
L_2	-10.1635	-9425.261	8.092	-18494.2620	-27909.360	10.19	46.1571
Mn-L_2	110722.631	101210.843	2.077	145897.817	136386.029	1.017	323.064
Rh-L_2	113548.637	103971.541	1.36	133647.951	124070.863	1.288	327.032
Pd-L_2	96926.87	87421.77	1.812	140706.71	131201.619	3.082	110.556
L_3	-32.7872	-10548.261	7.854	-20666.3135	-31181.787	10.5	47.2726
Mn-L_3	128884.701	118272.537	1.234	131947.329	121335.165	1.343	272.517
Rh-L_3	121533.701	110856.238	1.774	138398.914	127721.45	1.663	265.145
Pd-L_3	-185.481	-10790.955	2.758	-21575.46	-32180.93	6.304	108.453

As indicated in Table 2, the semi-empirical (PM3) method can be used to estimate the total energy and dipole moment for all produced ligands using the program (Gaussian Gauss View Currently Available Versions 5.0.9).

Table 2. Total energy in (KJ. Mol^{-1}) and dipole moment in (Debye) calculated using the Gaussian software for all produced ligands.

Comp.	Total energy	μ
L_1	0.12753359	6.3793
L_2	0.12399370	8.6931
L_3	0.09678410	8.1826

(3-2) Theoretical Computation of Ligands Vibration Frequencies*:*

As indicated in Tables 3 to 5 for both programs, the PM3 technique was employed to predict the vibration spectra of the generated compounds because it is in perfect agreement with the experimental data [18]. One can use theoretical spectra created by quasi-empirical calculations to comprehend the observed peaks in the spectrum. We identified the vibrational peaks of free connections. Figures 1 to 3 show data from Hyperchem-8 and Gaussian, while Figures 4 to 6 show the results. The theoretical frequencies of the produced races deviate from the experimental findings in some ways. Errors or variances in frequency calculations can be caused by a number of variables, including the coupling of the vibration mode, the mismatch of large-amplitude vibration modes, and the approximation in which each normal mode of vibration interacts with the IR beam.

Table 3. Using the Gaussian and Hyper Chem-8 programs, the vibrational frequencies of L_1 were calculated.

Symb.	ν (C-H)Py.	ν (C-H) tri.	ν (N=N)	ν (C=N)Py.	ν (C-N)tri.	ν (C-O-C)
***Exp.**	3091.99	3136.36	1595.18	1508.38	1220.98	1122.61
Hyper.	3077.31 (0.48)	3100.55 (1.15)	1716.45 (-7.06)	1575.37 (-4.25)	1262.05 (-3.25)	1148.69 (-2.27)
Gass.	3078.50 (0.44)	3119.24 (0.55)	1715.35 (-7.01)	1578.69 (-4.50)	1272.06 (-4.02)	1136.04 (-1.18)

Table 4. Using the Gaussian and Hyper Chem-8 programs, the vibrational frequencies of L_2 were calculated.

Symb.	ν (C-H)Py.	ν (C-H) tri.	ν (N=N)	ν (C=N)Py.	ν (C-N)tri.	ν (C-O-C)
***Exp.**	3091.99	3138.29	1593.25	1503.25	1220.98	1122.61
Hyper.	3076.99 (0.49)	3122.36 (0.51)	1602.14 (-0.55)	1577.45 (-4.93)	1262.06 (-3.25)	1167.95 (-3.88)
Gass.	3078.52 (044)	3119.36 (0.61)	1604.66 (-0.71)	1578.69 (-4.78)	1274.01 (-4.16)	1134.76 (-1.07)

Table 5. Using the Gaussian and Hyper Chem-8 programs, the vibrational frequencies of L_3 were calculated.

Symb.	ν (C-H)Py.	ν (C-H) tri.	ν (N=N)	ν (C=N)Py.	ν (C-N)tri.	ν (C-O-C)
*Exp.	3093.29	3138.29	1595.18	1505.04	1220.98	1122.61
Hyper.	3060.67 (1.06)	3124.23 (0.45)	1600.67 (-0.34)	1562.15 (-3.65)	1259.00 (-3.01)	1130.63 (-0.71)
Gass.	3058.85 (1.13)	3119.39 (0.61)	1604.68 (-0.59)	1578.69 (-4.66)	1274.78 (-4.22)	1135.11 (-1.10)

Where:
*: Experimental frequency.
: Theoretical frequency.
( ): Error % due to main different in the experimental measurements and theoretical treatment of vibrational spectrum.

Symb.	HyperChem-8 Program	Gaussian Program
ν (C-H)Py.	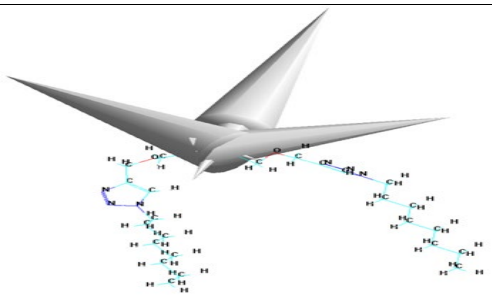	
ν (C-H) tri.	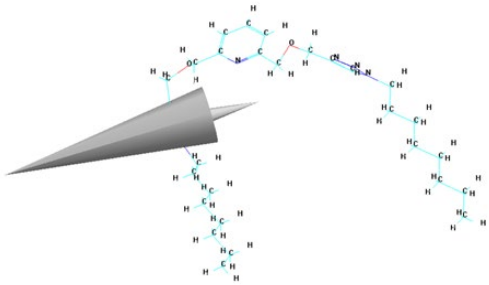	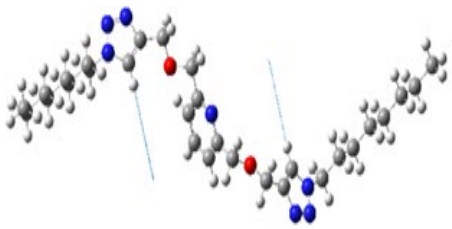
ν (N=N)	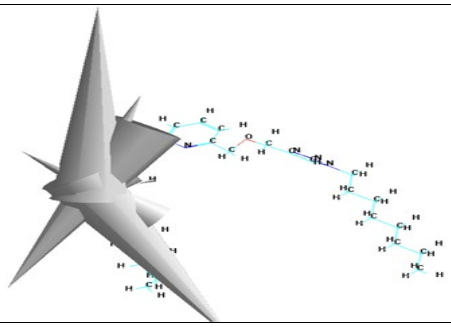	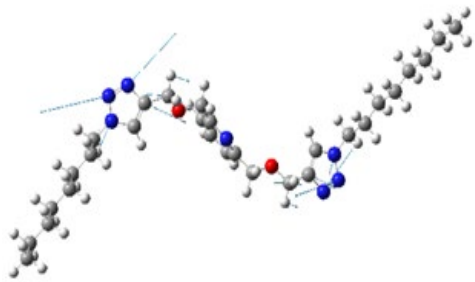
ν (C=N)Py.	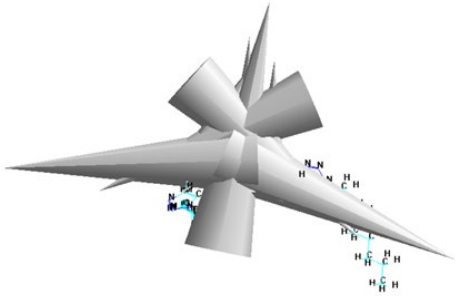	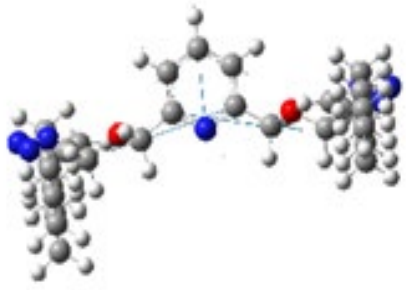

Fig. 1. HyperChem-8 and Gaussian programs were used to calculate the vibrational frequencies of (L_1).

Symb.	HyperChem-8 Program	Gaussian Program
ν (C-H)Py.	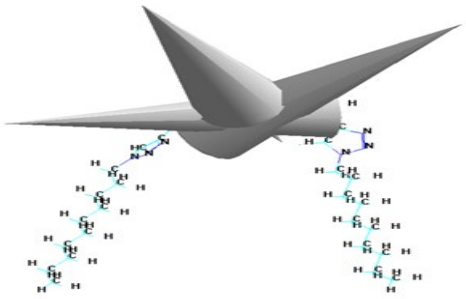	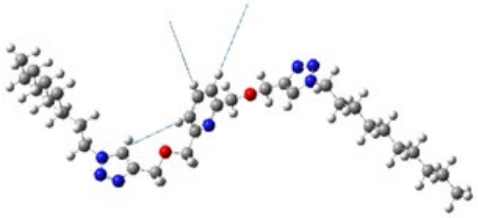
ν (C-H) tri.	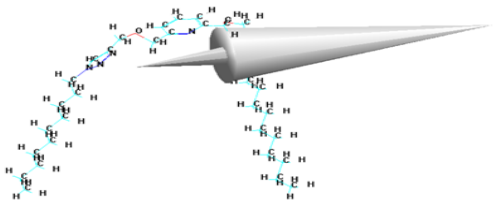	
ν (N=N)	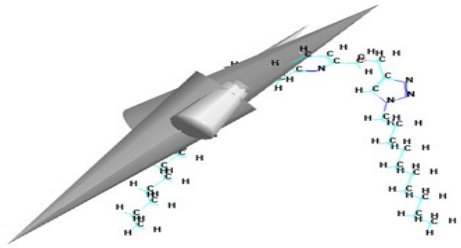	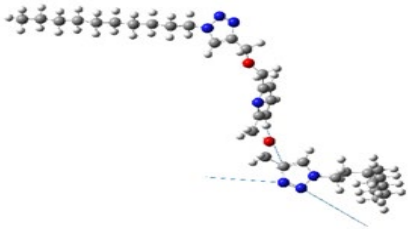
ν (C=N)Py.	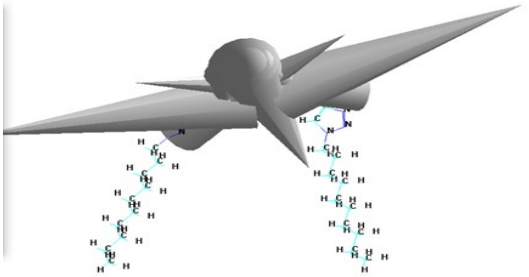	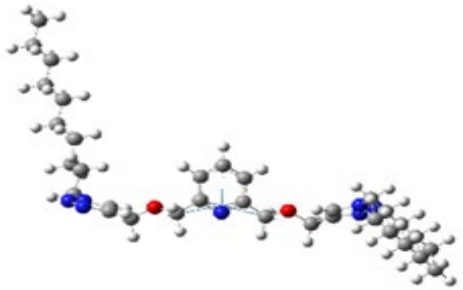

Fig. 2. HyperChem-8 and Gaussian programs were used to calculate the vibrational frequencies of (L_2).

Symb.	HyperChem-8 Program	Gaussian Program
ν (C-H)Py.	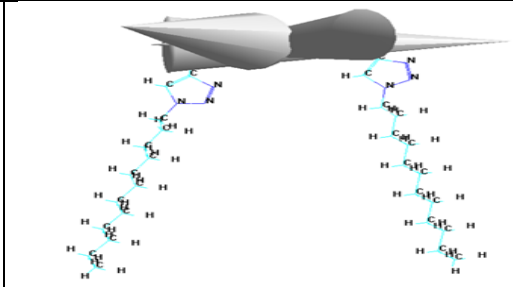	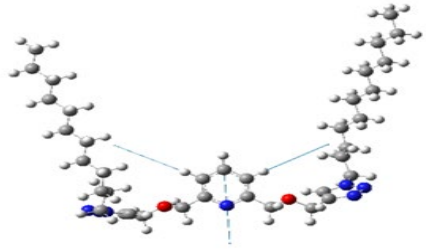
ν (C-H) tri.	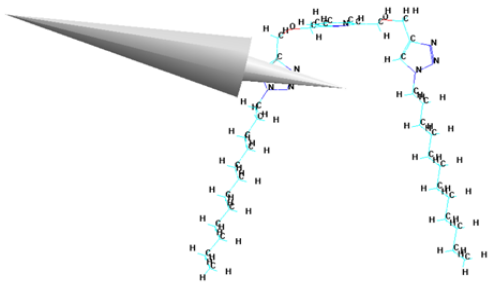	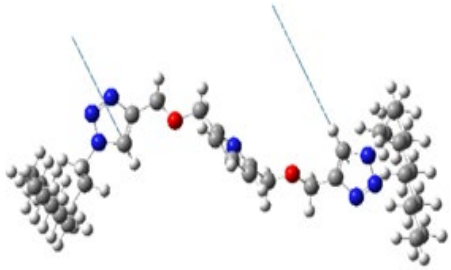
ν (N=N)	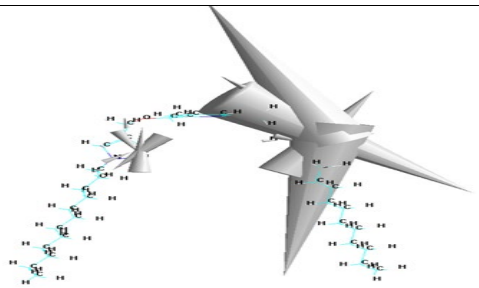	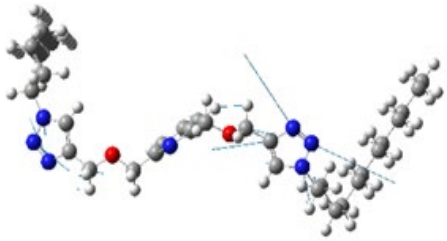
ν (C=N)Py.	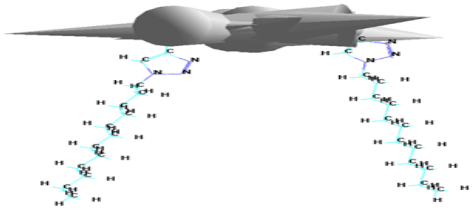	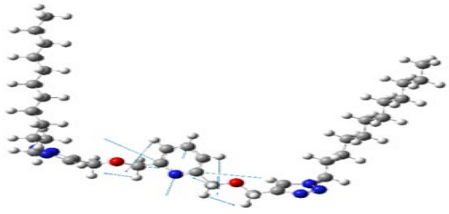

Fig. 3. HyperChem-8 and Gaussian programs were used to calculate the vibrational frequencies of (L_3)

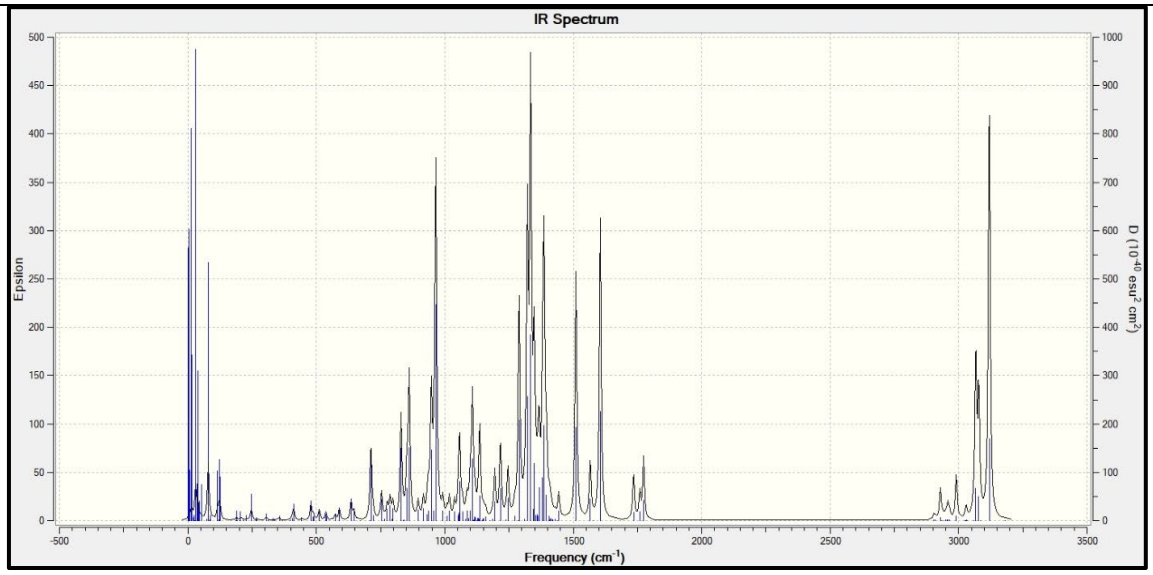

Fig.4. The vibrational frequencies of the molecules were calculated using the HyperChem-8 and Gaussian programs (L_1)

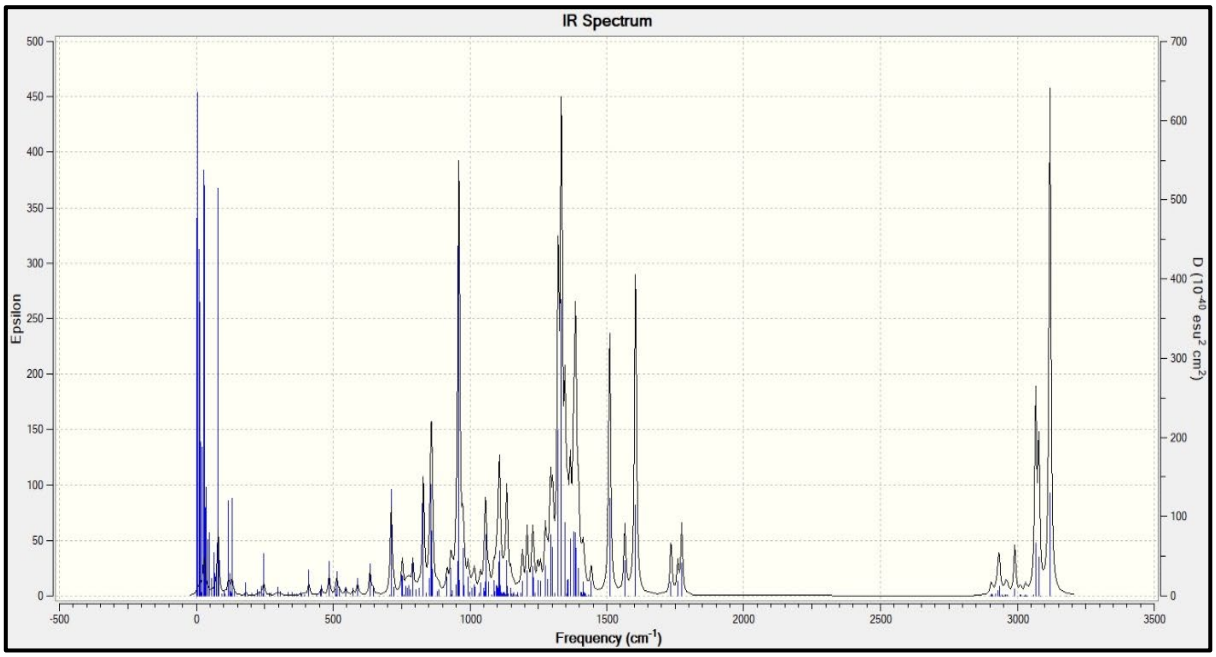

Fig. 5. The vibrational frequencies of the molecules were calculated using the HyperChem-8 and Gaussian programs (L_2)

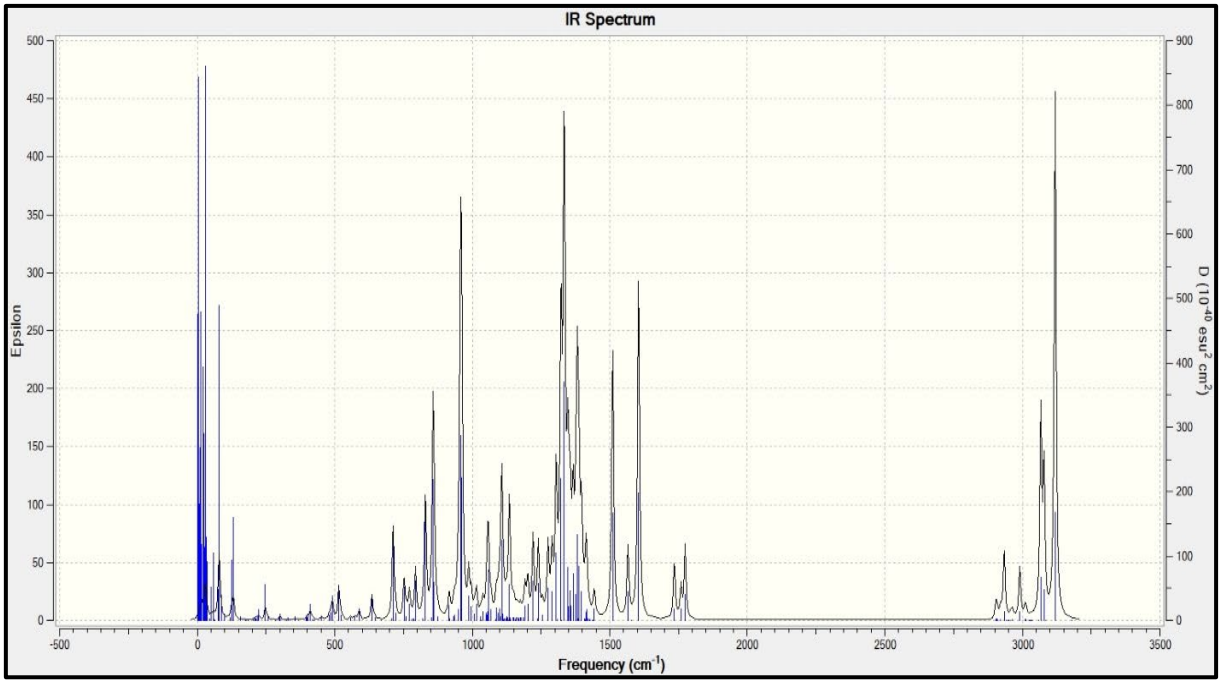

Fig. 6. The vibrational frequencies of the molecules were calculated using the HyperChem-8 and Gaussian programs (L_3)

(3-2) Theoretical Computation of Ligands Electronic Spectra:

The PM3 and ZINDO/S methods are used to compute the theoretical UV spectra of ligands. It revealed some differences from the experimental results, although these differences were typical for theoretical computations [19,20]. As shown in Figure 7, the kind of orbital and subsequent type of transition are determined by the serial number of atoms, which is drawn into the ligand structure. According to the ZINDOS method, the theoretical UV spectrum of the ligand L_1 exhibits three bands at 223.25, 243.72, and 257.70 nm due of the transitions $\pi \rightarrow \pi^*$ ($C_1 \rightarrow C_2$ or $C_5 \rightarrow C_6$), ($C_{10} \rightarrow C_{11}$ or $C_{26} \rightarrow C_{30}$) and $n \rightarrow \pi^*$ ($O_8 \rightarrow C_7$ or $O_8 \rightarrow C_9$ or $N_{12} \rightarrow C_{11}$ or $N_{14} \rightarrow C_{10}$ or $O_{24} \rightarrow C_{23}$ or $O_{24} \rightarrow C_{25}$ or $N_{27} \rightarrow C_{26}$ and $N_{29} \rightarrow C_{30}$) transitions respectively, as shown in Figure 8. for aromatic ring. While the experimental spectrum showed three bands at 237, 256 and 265 nm assigned to $\pi \rightarrow \pi^*$ and $n \rightarrow \pi^*$,

respectively. Three peaks at 232.59, 249.02, and 257.00 nm appeared in the theoretical spectra of L_2 by ZINDO's approach, respectively. due of the transitions π→π* (C_1→C_2 or C_5→C_6), (C_{10}→C_{11} or C_{26}→C_{30}) and n →π* (O_8→C_7 or O_8→C_9 or N_{12}→C_{11} or N_{14}→C_{10} or O_{24}→C_{23} or O_{24}→C_{25} or N_{27}→C_{26} and N_{29}→C_{30}) transitions respectively, as shown in Figure 9. while the experimental spectrum is about 254, 264, and 371nm assigned to π →π* and n→ π* respectively. Three bands were present in the theoretical spectrum of the ligand L3 at 223.97, 243.65, and 255.71 nm, respectively assigned to π →π* (C_1→C_2 or C_5→C_6), (C_{10}→C_{11} or C_{30}→C_{34}) and n→ π* (O_8→C_7 or O_8→C_9 or N_{12}→C_{11} or N_{14}→C_{10} or O_{28}→C_{27} or O_{28}→C_{29} or N_{31}→C_{30} and N_{33}→C_{34}) transitions respectively, Figure 10. while the experimental spectrum is about 219, 239, 265 nm attributed to π → π* and n→ π*. According to Table 6, all of the aforementioned data were acquired using the Hyperchem -8 application, while Gaussian program can provide (λ max) using a single point energy (SP) with ZINDO method for ligands by using type frequency (freq.) as represented in Table 7. For the three ligands respectively.

Table 6. Calculation of UV spectra of ligands using PM3 and ZINDOS and experimentation using the HyperChem-8 program

Symb.	Assignment Transition	Experimental (nm)	Theoretical ZINDO\S(nm)
L_1	n→ π* π → π*	265 256 237	257.70 243.72 223.25
L_2	n→ π* π → π*	371 264 254	257.00 249.02 223.59
L_3	n→ π* π → π*	265 239 219	255.71 243.65 223.97

Table 7. Comparison of experimental and theoretical electronic transitions for ligands using the Gaussian program and ZINDO calculations.

Symb.	Assignment transition	Experimental (nm)	Theoretical ZINDO (nm)
L_1	n→ π* π → π*	265 256 237	318 316
L_2	n→ π* π → π*	371 264 254	327 315 318
L_3	n→ π* π → π*	265 239 219	330 318 309

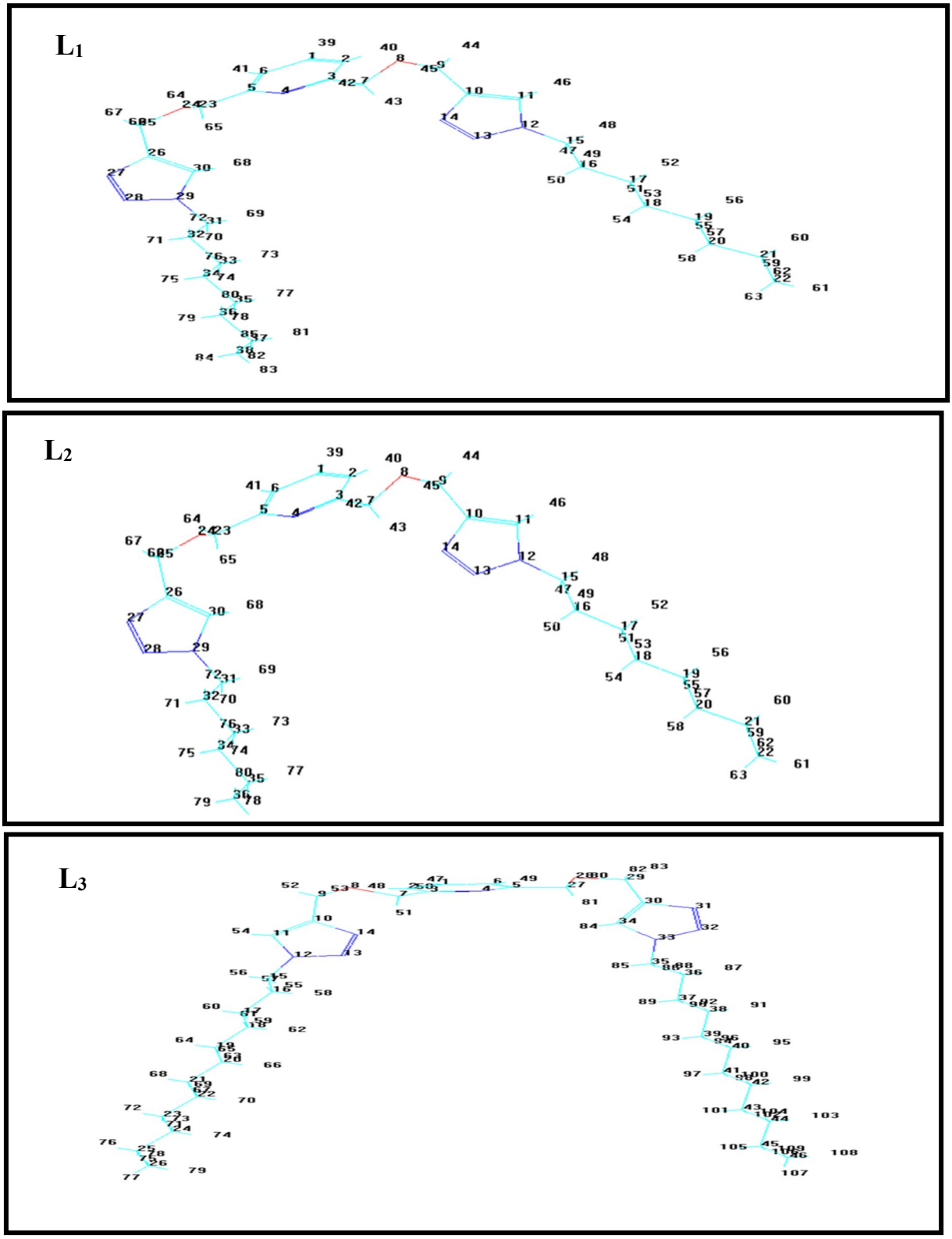

Fig.7. The number of atoms of ligands L_1, L_2 and L_3 using Hyper-chem8 program

HyperChem-8	ZINDO/S	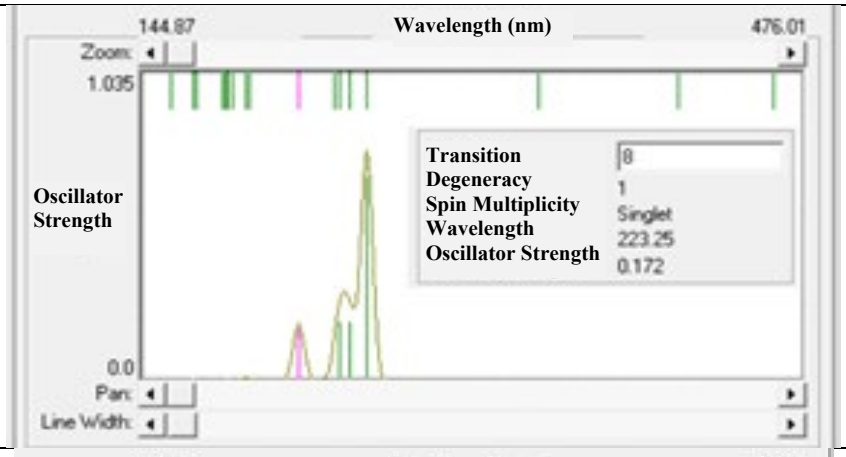	
		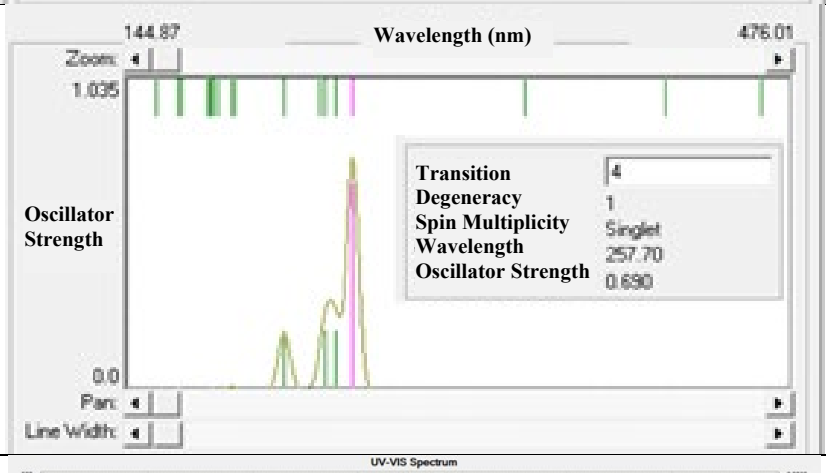	
Gaussian	ZINDO	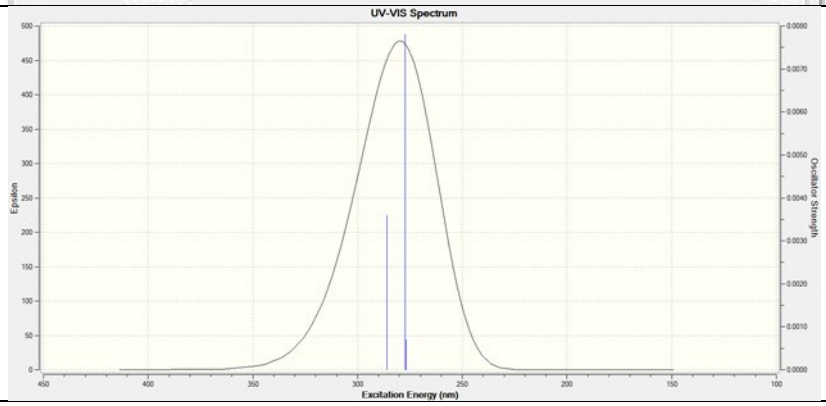	

Fig. 8. Theoretical uv –spectrum of ligand (L_1) using HyperChem-8 and Gaussian programs.

HyperChem-8	ZINDO/S	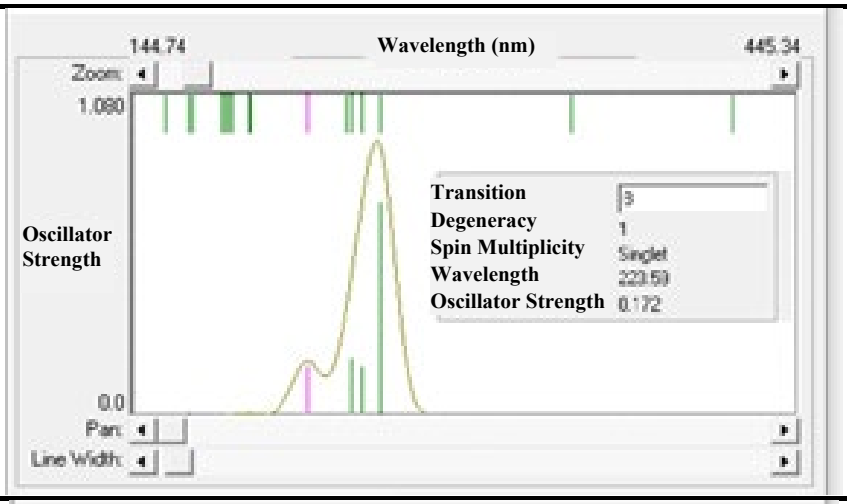
		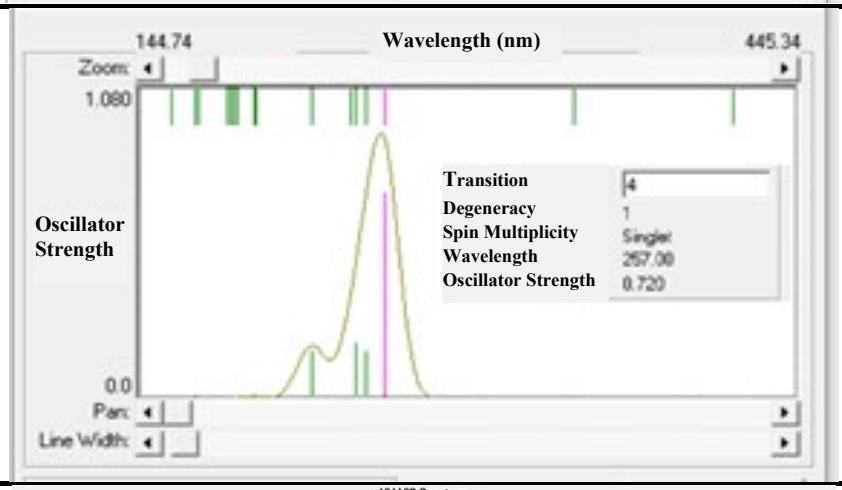
Gaussian	ZINDO	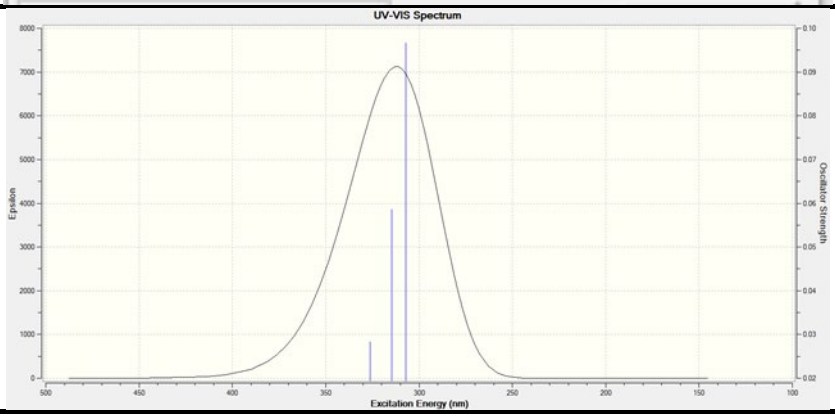

Fig. 9. Theoretical UV –spectrum of ligand (L_2) using HyperChem-8 and Gaussian programs.

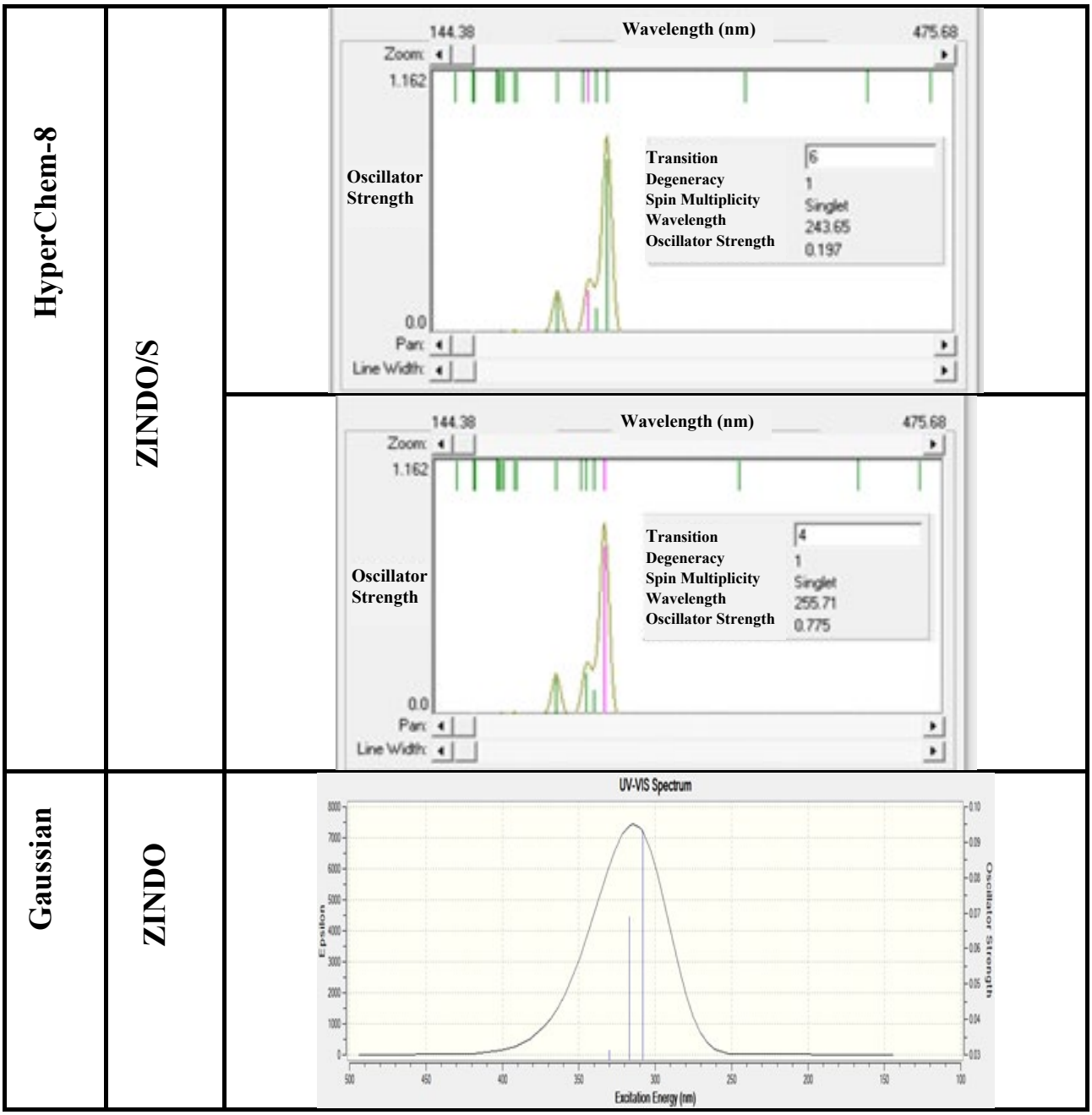

Fig.10. Theoretical UV –spectrum of ligand (L_3) using HyperChem-8 and Gaussian programs.

(3-3) Frontier Molecular Orbitals and Electrostatic Potential (E.P):

Further examination of the reactive bond locations to determine the electronic dispersion and electrostatic potential concentration based on the electronic density. The interaction of the energy molecule system with the positive point charge was characterized by the electronic potential (EP). To identify the reactive portions of the molecule, the E.P. of the connections is depicted in two and three dimensions [21].

Moreover, the stereochemistry and kinetics of various processes involving soft electrical materials and nucleophiles can be explained by boundary orbital characteristics (HOMO & LUMO). In many reactions, HOMO-LUMO interference serves as a control. The HOMO and LUMO values were displayed as a 3D counter to learn more about these compounds [22]. As seen in Figures 11 and 12, the LUMO of transition metal ions prefers to interact with the HOMO of the donor atoms in the bonds that are created. utilizing the Gaussian program and Hyperchem-8.

E.P (L_1) in 2D	E.P (L_1) in 3D	HOMO&LUMO (L_1) in 2D	HOMO & LUMO (L_1) in 3D
E.P (L_2) in 2D	E.P (L_2) in 3D	HOMO & LUMO (L_2) in 2D	HOMO & LUMO (L_2) in 3D
E.P (L_3) in 2D	E.P (L_3) in 3D	HOMO & LUMO (L_3) in 2D	HOMO & LUMO (L_3) in 3D

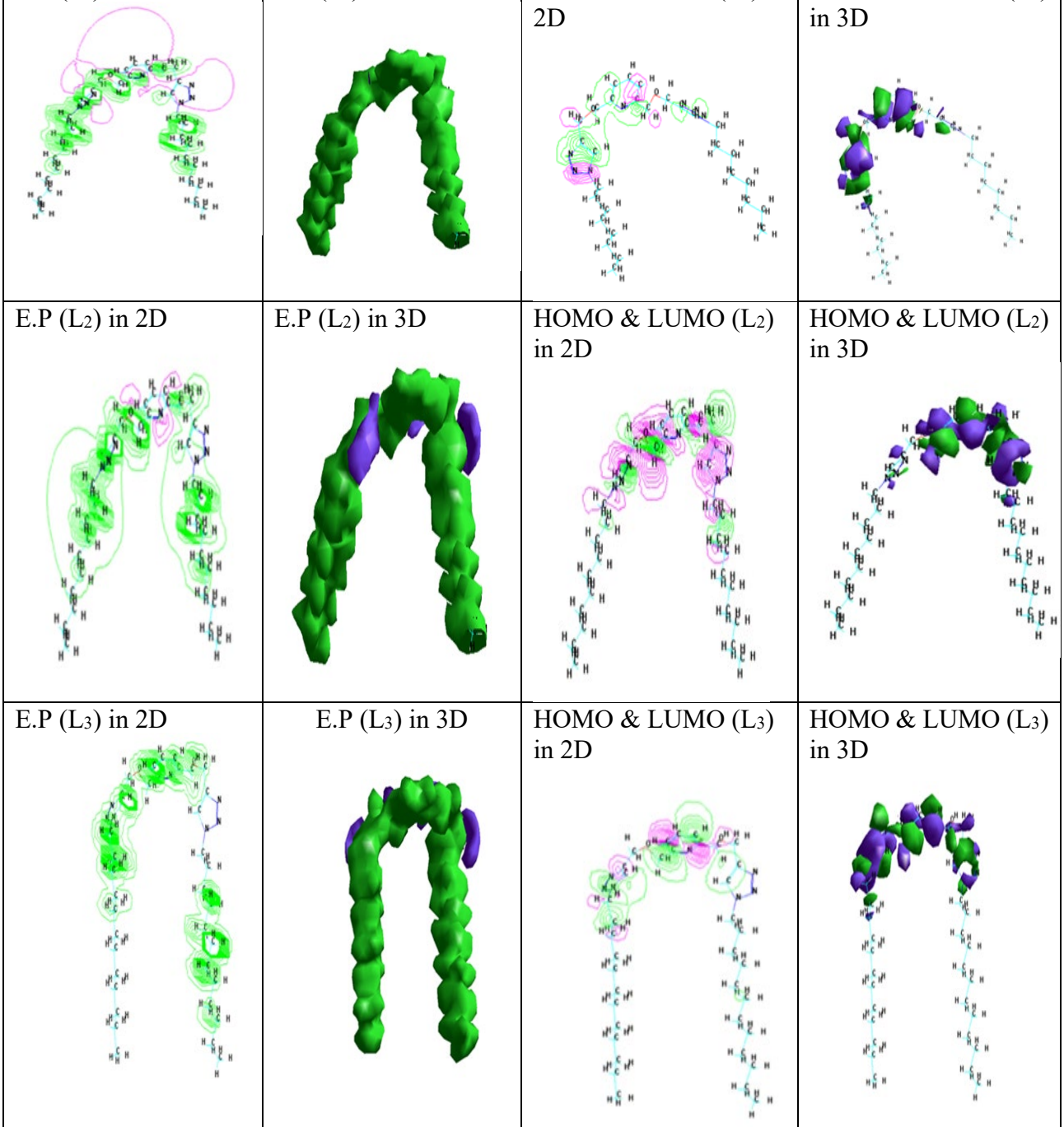

Fig. 11. HOMO& LUMO and Electrostatic potential as 2& 3D counters for Ligands by Hyperchem-8 program

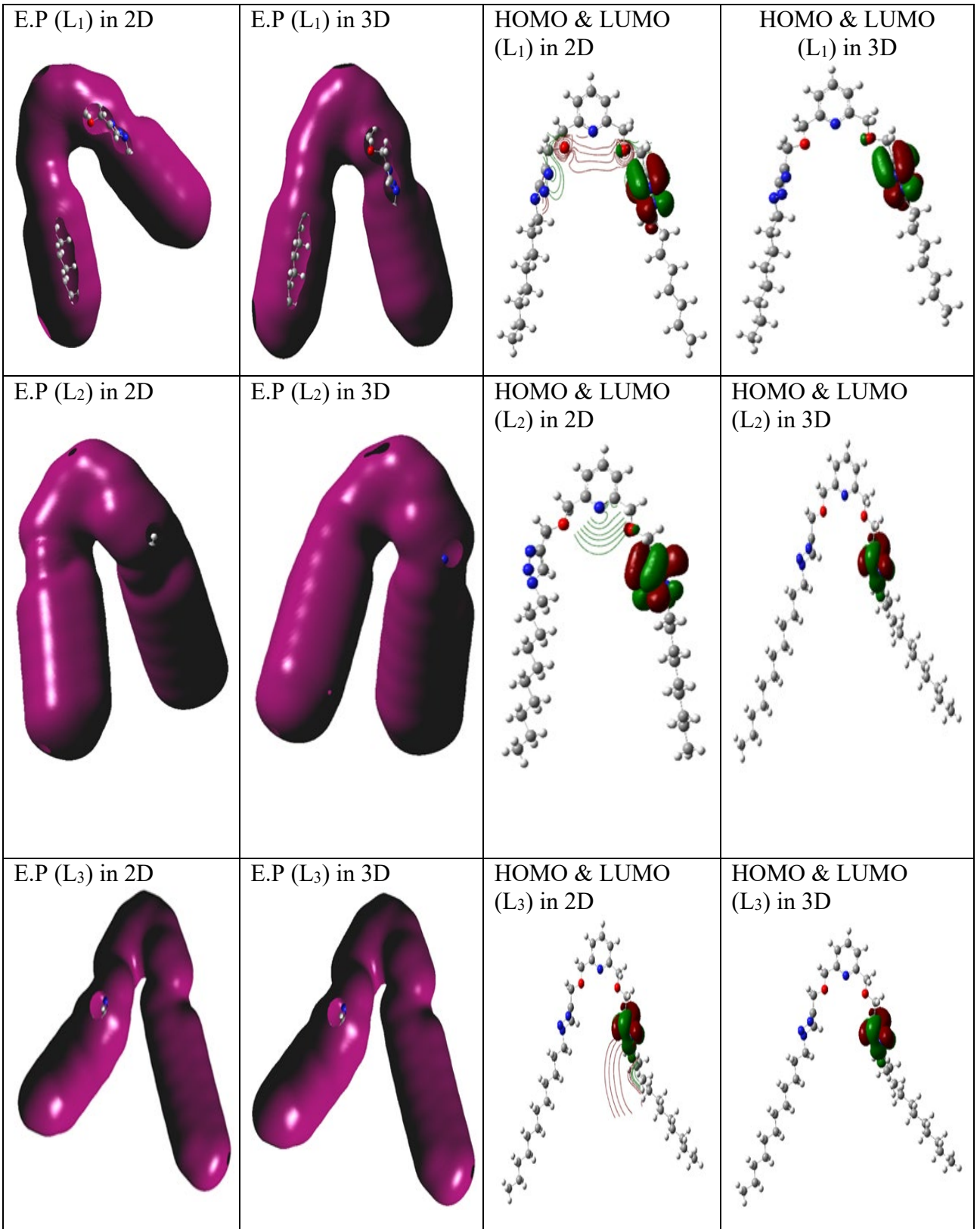

Fig. 12. HOMO& LUMO and Electrostatic potential as 2& 3D counters for Ligands by Gaussian program.

References

[1] Ibraheem, I. H. *et al.* (2022) 'Synthesis, Spectral Identification, Antibacterial Evaluationand Theoretical Study of Co, Fe, Rh and Pd Complexes for 2-benzoylthiobenzimidazol', *Baghdad Science Journal*, 19(6), p. 1326.

[2] LeMaitre, P. A. and Thompson, R. B. (2023) 'Gaussian basis functions for an orbital-free-related density functional theory of atoms', *International Journal of Quantum Chemistry*, p. e27111.

[3] Melander, M. M. *et al.* (2019) 'Grand-canonical approach to density functional theory of electrocatalytic systems: Thermodynamics of solid-liquid interfaces at constant ion and electrode potentials', *The Journal of chemical physics*, 150(4), p. 41706.

[4] Kumar, C. R. S. (2019) 'Approach of Density Functional Theory to Molecules Using Gaussian', *International Journal of Pure and Applied Physics*, 15(1), pp. 1–13.

[5] Ghulam, S. A., AL-Kaabi, M. A. and Rasool, W. S. (2022) 'Theoretical study of diallyl phthalate using density functional theory', in *AIP Conference Proceedings*. AIP Publishing LLC, p. 30023.

[6] Abdulameera, J. H. and Alias, M. F. (2022) 'Synthesis and characterization of some metal complexes with 2, 6-bis (((1-octyl-1H-1, 2, 3-triazol-4-yl) methoxy) methyl) pyridine and the study of their biological activities'. *Eurasian Chem. Commun*.4 p.1266-1284

[7] Abdulameer, J. H. and Alias, M. F. (2022) 'Synthesis, Characterization and Antimicrobial Activity of Cu(II), Pt(IV) and Au(III) Complexes with 2,6-bis(((1-decyl-1H-1,2,3- triazole-4-yl)methoxy)methyl)' pyridine. *Chemical Methodologies*, 6(3), p. 184-196.

[8] Abdulameer, J. H. and Alias, M. F. (2022) Heavy Metal Complexes of 1, 2, 3-Triazole derivative: Synthesis, Characterization, and Cytotoxicity Appraisal Against Breast Cancer Cell Lines (MDA-MB-231). *Baghdad Science Journal*, 19(6), p. 1410-1422.

[9] Alias, M., Ismael, S. and Abd Mousa, S. (2015) 'Synthesis, Characterization and Theoretical Study of Some Mixed-ligand Complexes of 2-Quinoline Carboxylic Acid and 4, 4⁄-dimethyl, 2, 2⁄-Bipyridyl with Some Transition Metal Ions', *Al-Nahrain Journal of Science*, 18(1), pp. 28–38.

[10] Abdullah, S. A. H. *et al.* (2017) 'Theoretical Study and Biological Activity of Co (II), Ni (II), Cu (II), Pd (II), Pt (IV) and Cd (II) Complexes with2-Thioxoimidazolidin-4-one Derivative', *Al-Mustansiriyah Journal of Science*, 28(2), pp. 64–72.

[11] Al-Hasani, R. A. A., Abed, A. H. and Ibrahim, S. K. (2016) 'Synthesis, Characterization, Theoretical Studies and Bioactivity of Pd (II), Rh (III), Ru (III) and Pt (IV) Complexes with 1, 8-Naphthalimide Derivative', *Iraqi Journal of Science*, 57(4B), pp. 2575–2591.

[12] Al-Dulimia, A. A. A., Al-Hasani, R. A. M. and Yousif, E. A. (2016) 'Synthesis, characterization, theoretical studies and photostabilization of mefenamic acid derivative with some divalent metal ions', *EUROPEAN CHEMICAL BULLETIN*, 5(10), pp. 456–464.

[13] Fereidoonnezhad, M. *et al.* (2018) 'Cycloplatinated (II) complexes bearing an O, S-heterocyclic ligand: search for anticancer drugs', *New Journal of Chemistry*, 42(9), pp. 7177–7187.

[14] Fereidoonnezhad, M. *et al.* (2017) 'Cyclometalated platinum (II) complexes bearing bidentate O, O′-Di (alkyl) dithiophosphate ligands: photoluminescence and cytotoxic properties', *Organometallics*, 36(9), pp. 1707–1717.

[15] Barwiolek, M. *et al.* (2022) 'Experimental and Theoretical Studies of the Optical Properties of the Schiff Bases and Their Materials Obtained from o-Phenylenediamine', *Molecules*, 27(21), p. 7396.

[16] Anbazhakan, K. *et al.* (2020) 'Theoretical assessment of antioxidant property of polyproponoid and its derivatives', *Structural Chemistry*, 31, pp. 1089–1094.

[17] Najim, Z. A. (2021) 'Molecular Docking, Electronica, Structural Characterization of Xanthanolides Derivative A: PM3 Model and ADMET.', *Egyptian Journal of Chemistry*, 64(7), pp. 3457–3463.

[18] Da-yang, T. E. *et al.* (2023) 'Structures, binding and clustering energies of Cu^{2+} (MeOH) n= 1-8 clusters and temperature effects: A DFT study', *Polyhedron*, 234, p. 116343.

[19] Panigrahi, P. *et al.* (2020) 'Improved adsorption and migration of divalent ions over C4N nanosheets: potential anode for divalent batteries', *Surfaces and Interfaces*, 21, p. 100758.

[20] Deshpande, S. S. *et al.* (2021) 'Carbon Nitride Monolayers as Efficient Immobilizers toward Lithium Selenides: Potential Applications in Lithium–Selenium Batteries', *ACS Applied Energy Materials*, 4(4), pp. 3891–3904.

[21] Hussain, T. *et al.* (2020) 'Functionalized two-dimensional nanoporous graphene as efficient global anode materials for Li-, Na-, K-, Mg-, and Ca-ion batteries', *The Journal of Physical Chemistry C*, 124(18), pp. 9734–9745.

[22] Ali, M. *et al.* (2020) 'Influence of organic acid concentration on wettability alteration of cap-rock: implications for CO_2 trapping/storage', *ACS applied materials & interfaces*, 12(35), pp. 39850–39858.